Article

Characterizing MIMO Channels in Low-Voltage Electric Power Line Communication Through Impedance and Scattering Parameters Analysis

Matheus C. de Sousa[1] , Wesley M. Cantarino[1] , Luís G. da S. Costa[1] , Thales A. Curty[1] ,
Daniel A. B. Fonseca[1] , Ulysses R. C. Vitor[1] , Marcelo E.V. Segatto[2]

[1]*Department of Electrical Circuit, Federal University of Juiz de Fora, 36036-900 Juiz de Fora, MG, Brazil,*
emails:matheus.cabral@engenharia.ufjf.br, wesley.cantarino@engenharia.ufjf.br,
luis.guilherme@engenharia.ufjf.br, thales.curty@engenharia.ufjf.br, daniel.fonseca@engenharia.ufjf.br,
ulysses.vitor@engenharia.ufjf.br.
[2]*Universidade Federal do Espirito Santo, Vitoria, Espirito Santo, Brazil, marcelo.segatto@gmail.com*

Abstract— **This study examines the characteristics of the low-voltage MIMO-PLC electric power line channel, which operates within the 2-100 MHz frequency range. The research involved measurements in four different Setups using 2.5 mm copper wires, including phase, neutral, and protective earth wires. These wires were transposed within a conduit, measured in pairs, with variations in the number and lengths of branches, assuming a deterministic modeling behavior of the electric power line. Throughout the experimentation process, essential parameters such as the magnitude of the S_{21} scattering parameters and VSWR identify frequency ranges suitable for efficient data transmission. The findings suggest remarkable prospects for enhancing PLC communication across MIMO channels. Depending on the combination of cable lines, over 70% of the bandwidth remains available. Additionally, the overall average impedance measured at $77.14\,\Omega$ is vital for impedance matching in PLC coupling circuit designs.**

Index Terms— MIMO-PLC, power line communication, scattering parameter, impedance matching.

I. INTRODUCTION

In the realm of wireless communication, extensive research has focused on leveraging multiple-input multiple-output (MIMO) technology to enhance data transmission speed and capacity [1]. Additionally, advancements in standards and technology have paved the way for sophisticated signal processing and improved transmission methods. These innovations leverage existing network infrastructure and expand bandwidth, resulting in significantly higher data rates. It ensures transmission speeds reach gigabit-per-second levels at the physical layer [2]. However, the adoption of MIMO technology in power line communication (PLC) has gained significant attention from researchers because the performance of PLC systems has several limitations, including electrical noise, signal attenuation over long distances, and impedance mismatching [3]. Integrating MIMO technology into PLC presents a promising opportunity to achieve greater channel capacity, broader system coverage, and enhanced reliability in challenging environments. Specifically, employing MIMO technology for PLC become a viable alternative to

numerous broadband communication technologies, aligning with the trend of innovative solutions such as collecting the data of industrial electricity information, Smart Homes, internet of things (IoT), and Smart Grids [4], [5].

The performance of the PLC channel is degraded due to the presence of the impedance mismatch between the PLC coupling circuit and the electric power line [6]. To design and develop a robust and reliable communication system of reasonable complexity, it is important to understand the frequency-dependent characteristics of a dynamic electric power line channel. An impedance mismatch between the PLC coupling circuit and the electric power line leads to coupling losses, which significantly block the propagation and limit distance coverage of PLC signals [7]. In the study referenced by [8] the feasibility of implementing Broadband PLC is thoroughly examined through measurements conducted on a medium voltage network de-energized. The MIMO PLC network is characterized in the frequency range of 2-30 MHz, considering various phase combinations to identify the best and worst-case scenarios. Different from the paper [8] the measurements of this paper are conducted with the electric power line energized.

To investigate the impedance characteristic of the energized electric power line, we adopt the voltage standing wave ratio (VSWR) and S_{11} scattering parameters as a metric for evaluating impedance matching. Additionally, we examine transmission losses using the magnitude of the S_{21} scattering parameters. The measurement outcomes presented in this research were acquired from an experimental Setup, where we meticulously arranged three copper wires of 2.5 mm within a conduit. Typically, the electrical wiring within homes comprises three copper wires, namely phase (P), neutral (N), and protective earth (PE). The communication signals in existing in-home PLC systems only utilize the P and N wires. As a result, in-home PLC technology has been limited to a single-input single-output (SISO) configuration. Nevertheless, previous studies in [6] have introduced MIMO for single-phase in-home PLC. By incorporating the PE wire, multiple signal transmit/receive ports become available, including P-N, P-PE, and N-PE. It enables the development of a MIMO scenario that can effectively enhance the capacity of the PLC channel [9].

Compared with existing literature, the novelty of this article becomes evident. Unlike previous studies [10]–[13], which have largely concentrated on specific frequency ranges and configurations, this work takes an innovative approach by comprehensively measuring an exceptionally broadband spectrum from 2-100 MHz. The measurements culminate in the development of a reference modem featuring a carrier detection threshold, thereby establishing a novel benchmark for acceptable attenuation thresholds between transmitter-receiver PLC modems. Furthermore, the input impedance of the low-voltage (LV) electric power line was measured in nine different Cases. In other words, within the proposed MIMO network, there are nine possibilities of signal injection/reception. The analysis of transmission losses and bandwidth availability also contributes to advancing the effectiveness of broadband PLC systems.

This work presents a deterministic approach that combines impedance and magnitude of the S_{21} scattering parameter insertion loss analysis in LV energized Setups. It also conducts frequency band availability analyses, considering the sensitivity of a commercial PLC device. Another significant contribution of this study is the evaluation of electric power line impedance, providing valuable information for developing PLC coupling circuits.

The main findings of this study can be summarized as follows:

- The comprehensive assessment of the magnitude S_{21} scattering parameters and VSWR provides

valuable insights into signal transmission efficiency, attenuation, and impedance matching over the electric power line, respectively.

- The analysis of the S_{21} scattering parameters facilitated the identification of the available bandwidth to reliable signal transmission within the PLC system. System performance was evaluated relative to a predefined threshold of -22 dB, denoting the attainment of optimal signal integrity.

- A comparative analysis of four distinct electrical network Setups, each simulating different power outlets, allowed for the evaluation of the PLC system's performance across these configurations. This comparison sheds light on communication capabilities and limitations associated with each Setup.

- The study investigated the effects of branching on the PLC system's performance. The impact on impedance, attenuation, and available bandwidth was revealed by examining varying numbers of branches, providing valuable insights for system optimization.

The remainder of this paper is outlined as follows: Section II provides a comprehensive review of the most recent related works in the literature. Section III delves into the essential theory for understanding and modeling the electric power line. Sections IV and V present the results, along with their discussions and the conclusions derived from this study respectively.

II. LITERATURE REVIEW

This section provides a comprehensive literature review on the impedance and scattering parameters in LV MIMO PLC widely used to characterize the behavior of a transmission line (TL) and are essential in determining how signals propagate along the electric power line [14]. In the context of PLC MIMO [15], the input impedance becomes crucial for achieving efficient signal transmission and impedance matching between the PLC coupling circuits with the electric power line, both in narrowband applications up to 500 kHz [6] and broadband applications below to 100 MHz [16].

Impedance measurements conducted in Turkey across rural, urban, and industrial electric power lines in the frequency band of 10-170 kHz revealed significant variations in the impedance of the electric power line with frequency, indicating frequency-dependent behavior [17]. The impedance comprises not only resistance but also reactance, particularly inductive reactance [18], posing challenges for high-frequency small-signal transmission. Additionally, the impedance is significantly influenced by the electrical applications connected to the electric power lines, leading to time and location variations [19]. Consequently, achieving effective matching between PLC coupling circuits and the electric power line becomes a challenging task.

Several techniques have been developed to evaluate the impedance of electric and electronic circuits efficiently. [20]. These methods encompass a wide array of approaches, ranging from measuring current and voltage to employing balancing or resonating networks and network analysis. After all, not all these approaches lend themselves to straightforward implementation in a PLC modem for online operations [21].

In the study conducted by [22], accurate knowledge of input and load impedances in PLC is vital for optimizing smart grid design. The PLC channel's impedance, susceptible to unmatched loads, varies over time and frequency, leading to reduced power output and data rates between PLC modems. The study introduces a precise access impedance measurement system within the 30–500 kHz frequency range.

TABLE I. COMPARATIVE ANALYSIS OF KEY ASPECTS IN SCATTERING PARAMETERS AND MIMO PLC.

Aspect	Proposed paper	Baseline paper [4]	Baseline paper [7]	Baseline paper [15]
Research Objectives	Measurement of scattering parameters, VSWR, impedance and attenuation.	Line impedance and power quality estimation.	Facilitate the future MIMO PLC standardization the process by employing the appropriate channel models and contribute to forthcoming MIMO regulatory discussions through an extensive dataset of interference measurements.	Determine the impedance of the rural, urban and the industrial power lines.
Methodology	VNA measurements techniques.	Electronic boards currently used as on-field applications.	PLC modems and MIMO artificial Mains.	Signal generator and AC milivoltimeter.
Frequency Band	2-100 MHz	10 Hz-1 MHz	4-30 MHz	10-170 kHz
Impedance Analysis	Yes	Yes	Yes	Yes
Attenuation Measurements	Yes	Yes	Yes	Yes
MIMO System	Yes	No	Yes	No
Contributions and Novelty	Demonstrate the available bandwidth for communication between PLC modens. Characterize the behavior of an energized electric power line to efficiently design PLC coupling circuits and evaluate the scattering parameters behavior for four Setups.	Line impedance characterization using a single device capable of both characterizing the R–L characteristics of the line and generating the line-impedance frequency spectrum using non-parametric impedance estimation.	Explore the fundamentals of the channel model, encompassing the reception of common mode signals. This provides a preview of the imminent regulatory discussion, demonstrates the improvement in signal-to-noise ratio (SNR).	Presents some new empirical data on the impedance and attenuations of the electric power lines.

To facilitate a structured comparison, it is presented a detailed Table I juxtaposes the main characteristics of this paper with those of selected baseline papers. This comparative framework aims to highlight the distinctive contributions and innovations put forth in this work, offering readers a clear understanding of the advancements made within the context of existing literature. It has been considered a comprehensive analysis of key aspects in the domain of impedance analysis, scattering parameters, frequency band characterization, attenuation, and MIMO systems within electric power lines.

III. THEORETICAL MODELS OF THE LINE PARAMETERS

Effective PLC system design and analysis hinge on precise line parameter modeling. Several theoretical models exist to define line parameters that greatly influence PLC transmission. These models offer valuable predictions and insights into power line behavior within communication Setups. This section delves into prevalent theoretical models for electric power line parameters in PLC contexts.

In Fig. 1, we can observe an N-port network, where $V_N{}^+$ denotes the amplitude of the voltage wave incident on port n, and $V_N{}^-$ represents the amplitude of the voltage wave reflected from port n. The scattering matrix $[S]$ is defined based on these incidents and reflected voltage waves [23].

$$\begin{bmatrix} V_1^- \\ V_2^- \\ \vdots \\ V_N^- \end{bmatrix} = \begin{bmatrix} S_{11} & S_{12} & \cdots & S_{1N} \\ S_{21} & S_{22} & \cdots & S_{2N} \\ \vdots & \vdots & \ddots & \vdots \\ S_{N1} & S_{N2} & \cdots & S_{NN} \end{bmatrix} \begin{bmatrix} V_1^+ \\ V_2^+ \\ \vdots \\ V_N^+ \end{bmatrix} \tag{1}$$

where,

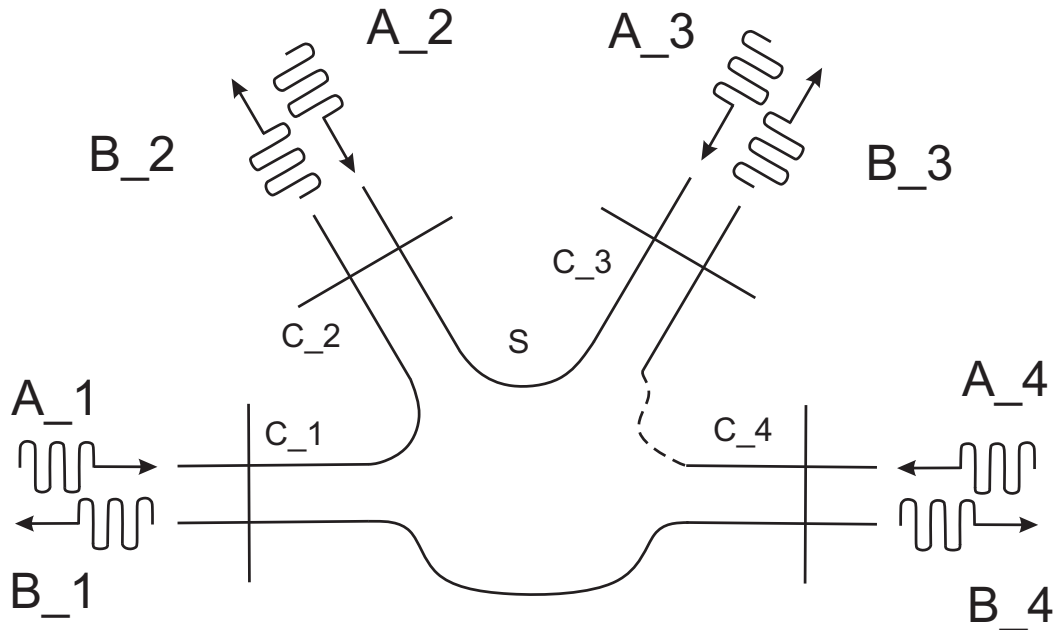$$S_{ij} = \frac{V_i^-}{V_j^+} |V_k^+ = 0 \; para \; k \neq j. \tag{2}$$

Fig. 1. An arbitrary N-port microwave network.

The broadband PLC signal propagates in the transverse electromagnetic mode (TEM) in the electric power line, where traditional TL theory finds extensive application in PLC systems, as covered extensively in the electromagnetic literature [23], [24]. The modeling of electrical circuits is essential in analyzing a TL within PLC systems. This modeling incorporates parameters such as resistance per unit length (R in Ω/m), capacitance per unit length (C in F/m), inductance per unit length (L in H/m), and conductance per unit length (G in ℧/m) [25], [26].

Considering the three lines in the propagation direction along the electric power line (i.e., z-direction), we can derive a model for an infinitesimal segment (Δs) of the line within an electromagnetic framework, as depicted in Fig. 2. Furthermore, for wires P and N, an equivalent TL model can be established,

where Req, Leq, Ceq, and Geq correspond to the equivalent resistance, inductance, capacitance, and conductance, respectively.
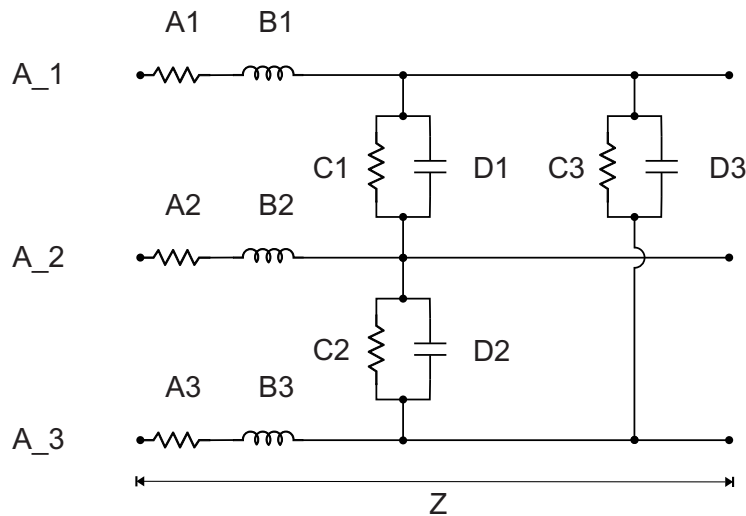

Fig. 2. Transmission line equivalent circuit for three wires.

The input impedance of the electric power line is typically a complex quantity that depends on various factors, such as the physical properties of the electric power line, its length, branches, and the frequency spectrum at which the signals propagate [27]. This impedance can vary due to the line's distributed parameters, such as capacitance, inductance, and loads, causing frequency and time-dependent variations. These fluctuations can lead to signal reflections and distortions, potentially affecting the performance of the PLC system [28]. As a result, designing the impedance of a PLC coupling circuit to inject and extract the PLC signal from the electric power line becomes feasible [29]. The impedance of an electric power line can be obtained from the two-port network S_{11} and S_{22} scattering parameters, which can be calculated by

$$Z_{in} = 50 \left(\frac{1 + S_{11}}{1 - S_{11}} \right). \tag{3}$$

All the measurements were conducted in a three-wire system comprising P, N, and PE. When injected into P, a signal induces a current in both N and PE. This characteristic remains consistent across all three wires within the system and, consequently, must be considered in modeling the TL. Moreover, the analyzed LV PLC electric power line can be treated as a network with six network ports, where three ports serve as inputs and the remaining three act as outputs [30]. These ports are combinations of two wires. As a result, both the input and output of the network ports offer three possibilities for signal injection (three combinations of two), as illustrated in Fig. 3.
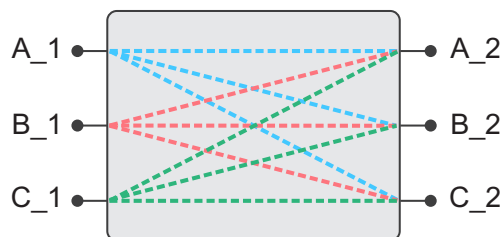

Fig. 3. Scheme of three wires MIMO modes.

To carry out measurements on the energized LV electric power line, the use of PLC coupling circuit is necessary to eliminate the mains frequency. The testing methodology and calibration process are explained in Section IV. It's important to note that during the calibration of the vector network analyser (VNA), the PLC coupling circuit, connectors, and cables were included in the calibration process to avoid distortion in the measurements of scattering parameter and impedance values of the PLC channel. The measurements were taken in the afternoon, with a temperature of approximately 30°C. For a 15 m line, this represents a variation of approximately 4.3% in the total resistance of the line when utilizing the linear thermal expansion approximation, as shown in Eq. 4 [31],

$$\rho = \rho_0 \left[1 + \alpha_{cu} \left(T - T_0 \right) \right], \tag{4}$$

where $\alpha_{cu} = 0.00429°\text{C}^{-1}$ represents the resistive temperature coefficient of the cooper and the resistivity of a cooper at 20°C is 1.724×10^{-8} Ω.m and conductivity is $5.95 \times 10^7/\Omega$.m [25]. Nevertheless, for minor temperature fluctuations of up to 2°C at 30°C, the variation amounts to just 0.85%. Consequently, these fluctuations were not factored into our results.

In recent years, the application of MIMO technology has garnered significant attention in various fields, including PLC. Within the domain of electric power lines, the integration of MIMO techniques shows promise for revolutionizing PLC. Traditionally, PLC has predominantly relied on single-phase systems. On the other hand, the escalating demand for higher data rates and more reliable communication has stimulated the exploration of MIMO concepts in the domain of three-wire electric power lines [32]. By capitalizing on the inherent characteristics of the three-wire electric power grid, particularly the interaction between wires P, N, and PE, a MIMO system can be designed to exploit spatial diversity, enhance channel capacity, and mitigate interference. This potential opens up exciting possibilities for bolstering the efficiency and reliability of communication networks operating over the electric power line infrastructure, represented by the matrix H [33].

$$H = \begin{bmatrix} h_{11} & h_{12} & \cdots & h_{1N_T} \\ h_{21} & h_{22} & \cdots & h_{2N} \\ \vdots & \vdots & \ddots & \vdots \\ h_{N_R1} & h_{32} & \cdots & h_{N_RN_T} \end{bmatrix}, \tag{5}$$

where N_T is the number of transmit ports, N_R is the number of the receive ports, and h_{nm} is the complex channel coefficient from transmit port m (m = 1, ..., N_T) to receive port n (n = 1, ..., N_R) for each frequency measurement point.

In Fig. 3, nine possible Setups are depicted, considering the injection of signals in the electric power line represented by P1, N1, and PE1, and the reception at the other end represented by P2, N2, and PE2. The measurements obtained from the VNA are denoted as 1 to 3 for the input port of the signals, corresponding lines P1 to PE1, respectively, and similarly, 4 to 6 for the output port of the measured signals from P2 to N2, respectively. Table II illustrates the complete set of measured port configurations for Cases 1 to 9, resulting from the preceding pairwise combinations.

Thus, the H matrix can be obtained from the transmission scattering parameters using the VNA, where C_i corresponds to the various Setup Cases listed in Table II, with i ranging from 1 to 9 in three lines Setup.

TABLE II. POSSIBLE COMBINATIONS FOR THE SYSTEM'S PORTS.

Setup	Input Port	Output Port
Case 1	P1N1	P2N2
Case 2	P1N1	P2PE2
Case 3	P1N1	N2PE2
Case 4	P1PE1	P2N2
Case 5	P1PE1	P2PE2
Case 6	P1PE1	N2PE2
Case 7	N1PE1	P2N2
Case 8	N1PE1	PE2P2
Case 9	N1PE1	N2PE2

$$H = \begin{bmatrix} S_{21}^{C_1} & S_{21}^{C_2} & S_{21}^{C_3} \\ S_{21}^{C_4} & S_{21}^{C_5} & S_{21}^{C_6} \\ S_{21}^{C_7} & S_{21}^{C_8} & S_{21}^{C_9} \end{bmatrix}. \tag{6}$$

A. Vector Network Analyzer

VNA measures high-frequency components' electrical traits [34], transmitting a test signal through the device under test (DUT) and measuring its response. It measures scattering parameters, signal transmission and reflection, and other traits such as impedance and phase.

Calibrating the VNA is pivotal, ensuring the accuracy and reliability of the measurements and provide traceability, quality assurance, and reducing phase errors. It aligns the DUT input-output with the reference plane, counteracting losses from cables and connectors for precise measurements [35].

The calibration's compatibility is ensured through a purpose-designed calibration kit from the VNA manufacturer, meticulously tailored to their specific VNA model. This kit seamlessly integrates with the VNA's architecture, including frequency range, connectors, and impedance specifications, ensuring full compatibility and accurate calibration. Fig. 4 show the Rohde & Schwarz VNA FSH8, operating from 100 kHz up to 8 GHz, along with the ZV-Z21 50 Ω N-Type calibration kit.

A demonstration utilizing the Smith Chart of the VNA enhances calibration understanding. Notably, two 8 m RG-58 coaxial cables extend the VNA port to a PLC coupling circuit connected to the power cable. These cables and the PLC coupling circuit are integrated into the calibration process. Their inclusion compensates for cable characteristics and eliminates systematic errors, enhancing measurement accuracy and reliability. Fig. 5 visually highlights the impact of calibration on port 1 of the VNA open-circuit termination, connected via a coaxial cable.

IV. METHODOLOGY

Accurately understanding an energized electric power line's behavior is essential for efficient PLC coupling circuit design and grasping key parameters like average channel attenuation, root-mean-square delay spread, coherence time, and coherence bandwidth [36]. Moreover, the analysis of scattering parameters and impedance mismatching is crucial for assessing grid performance and identifying potential signal propagation issues. This study adopts a deterministic modeling approach, assuming the electric power line's behavior lacks randomness, treating the load as time-invariant and frequency-invariant [37]. Consequently, impedance, including resistive, inductive, and capacitive measurements, can be thoroughly examined.

Fig. 4. Vector Network Analyser and calibration kit.

To measure the VSWR and scattering parameters, tests were conducted using four different Setups with three copper wires of 2.5 mm each, arranged in a 15 m length and routed through a 20 mm diameter conduit, varying the number of branching. The length and dimensions of the wires were estimated based on the average areas of Brazilian residences, as reported in [38]. Fig. 6 depicts the Setups utilized in the experiments:

- Setup 1 does not have any branching.
- Setup 2 contains a 2 m branching located in point A a 5 m from VNA port 1.
- Setup 3 features a 3 m branching located in point B a 10 m from VNA port 1.
- Setup 4 shows the presence of a 2 m branching located in point A at 5 m from VNA port 1 and 3 m branching located in point B at 10 m from VNA port 1.

Fig. 7 displays the schematic of the capacitive broadband PLC coupling circuit used in the measurement Setup, along with the magnitude of S_{21} scattering parameters. The design of the PLC coupling circuit is originally intended to effectuate impedance matching from 50 Ω. The capacitor C_1 serves to effectively block the mains LV voltage (i.e., 127 Vrms/60 Hz) from the electric power line, functioning
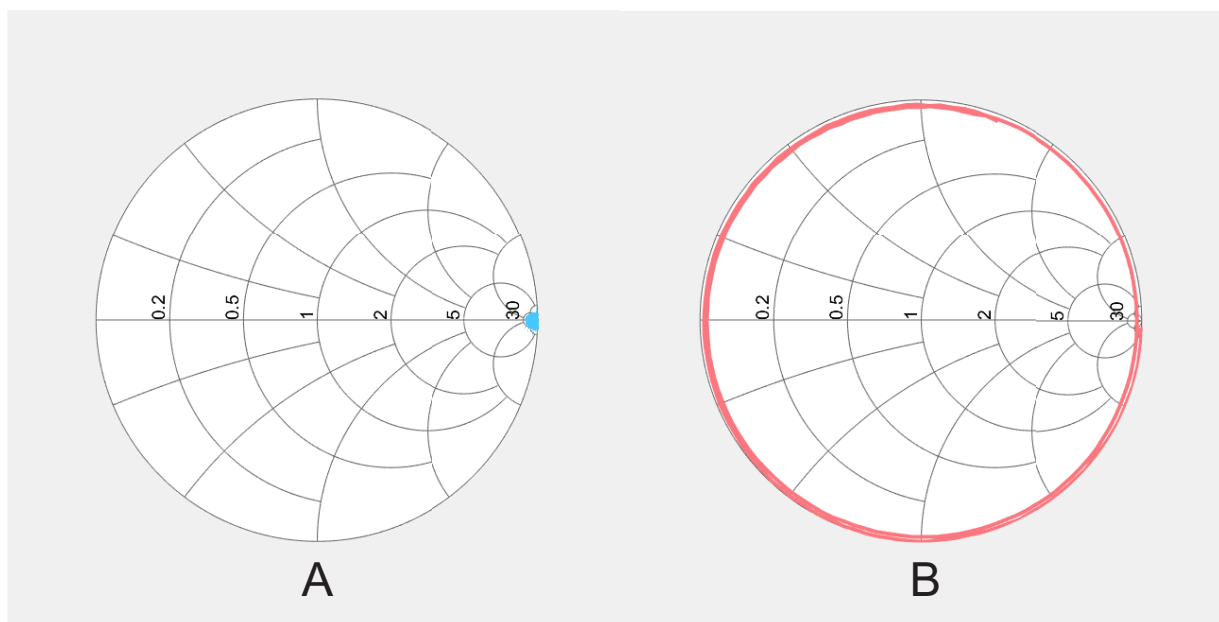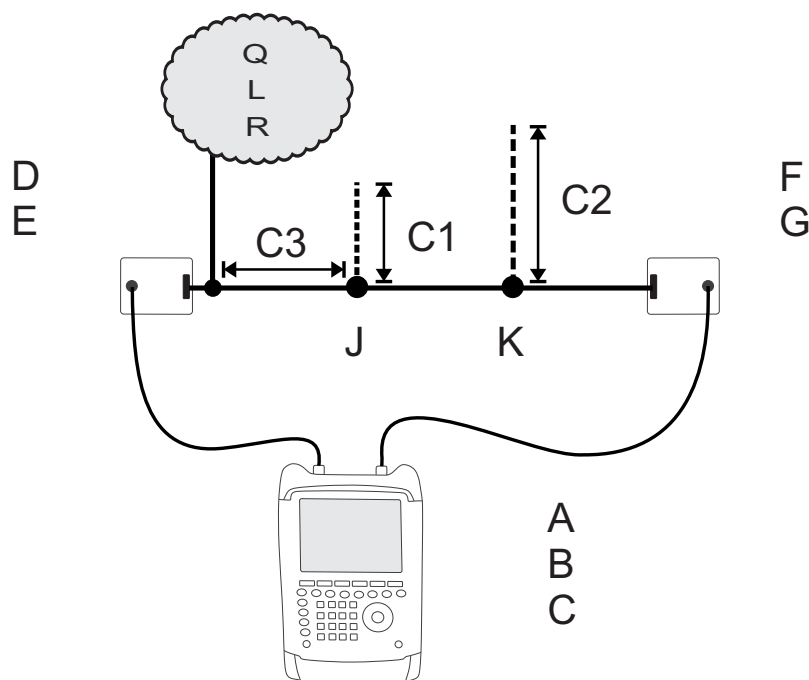
Fig. 5. Example of open calibration of VNA.

Fig. 6. Setup for measuring scattering parameters and input impedance at the electric power line.

as a first-order high-pass analog filter with a flat magnitude frequency response for frequencies higher than $f_l \geq 2\,\text{MHz}$. The $3\,\text{dB}$ cut-off frequency attenuation at $1\,\text{MHz}$ differs in both PLC coupling circuits due to the varying Capacitor C_1 values. In PLC coupling circuit #1, the magnitude of the S_{21} scattering parameters at $100\,\text{MHz}$ exhibit a loss of $1\,\text{dB}$, whereas in PLC coupling circuit #2, the loss is $1.8\,\text{dB}$. It is essential to note that the combination of capacitor C_1 and radio frequency (RF) transformer T_1 forms a band-pass filter operating within the frequency range of 1-$100\,\text{MHz}$. The RF transformer T_1 [39] ensures galvanic isolation between the VNA instrument and the electric power line, functioning as a balanced/unbalanced (BALUN) circuit that effectively separates the grounds of

the VNA instrument and the electric power line, as described in [40]. The passive components of the PLC coupling circuit are listed in Table III.

TABLE III. PASSIVE COMPONENTS OF PLC COUPLING CIRCUIT.

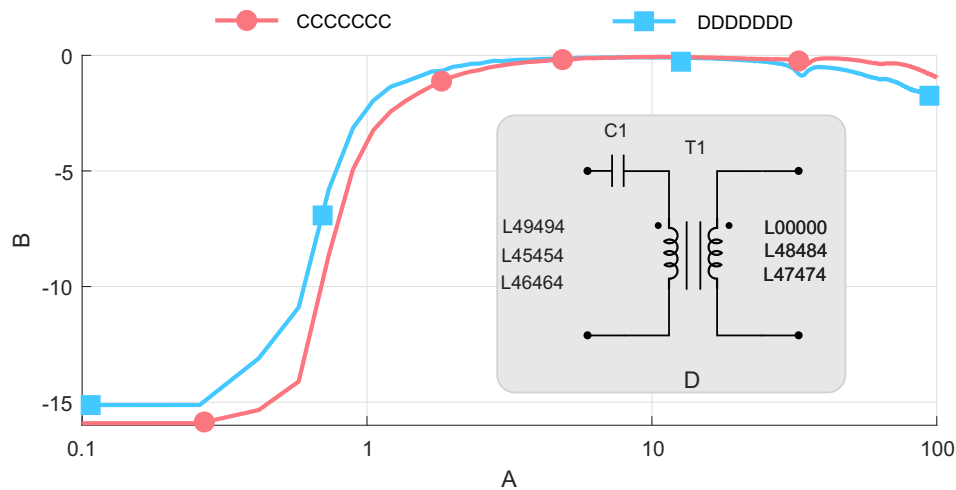| PLC coupling circuit	C_1 (nF)	T_1
#1	2.2	PWB 1010-1L
#2	3.3	PWB 3010-1L

Fig. 7. Magnitude of the S_{21} scattering parameter of PLC coupling circuit.

Before conducting measurements with a VNA, performing calibration is essential to ensure highly accurate and reliable results. A full port calibration was conducted on the two-port VNA, before measurements, to ensure accurate characterization of the device under test to evaluate the scattering parameters and VSWR, as shown in Fig. 6. During this step, VNA calibration involves characterizing and compensating for the systematic errors introduced by the measurement Setup, including the test cables, connectors, adapters, and PLC coupling circuit, as depicted in Fig. 8. The connectors used in the calibration process are listed accordingly in Table IV.
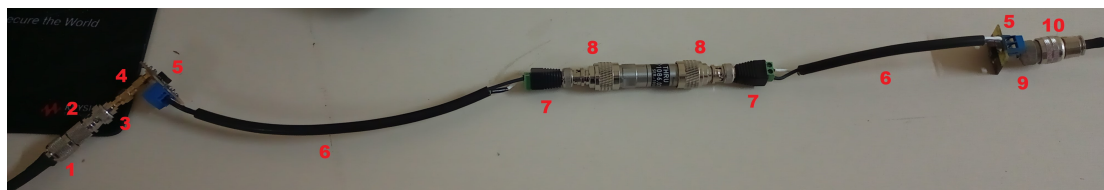
Fig. 8. Setup of measurement of scattering parameters of the electric power line.

The through calibration was performed following the previously discussed calibration steps (open, short, and load). The two-port standard used in this calibration is designed to connect two test ports directly. It is optimized to minimize loss and maintain a relatively short length. The characteristics of this standard, including loss and length, are typically accounted for within the analyzer itself. The through line is assumed to match the impedance used in the measurements closely. Impedance values were derived from S_{11} scattering parameter measurements obtained using the VNA. Specifically, Eq. 3

TABLE IV. COMPREHENSIVE RF ADAPTERS AND CONNECTORS USED IN CALIBRATION AND MEASUREMENT.

Item	Connector and adapter description
1	TNC male connector
2	Adapter TNC female to BNC female
3	Adapter BNC male to SMA female
4	Adapter SMA male to SMA male
5	PLC coupling circuit (SMA female and KRE)
6	Cooper wire 2.5 mm
7	BNC Screw Type Adapter Connector
8	Adapter BNC female to N male
9	Adapter SMA male to N female
10	N male connector

was used in the impedance analysis process, where numerical analysis software was used to calculate impedance values based on the measured S_{11} scattering parameter.

When evaluating the performance of a PLC modem, an essential factor to consider is the threshold received power. This parameter is used to determine the reliability and quality of the communication link. Gateways, such as [41], are capable of transmitting with a power spectral density (PSD) of -50 dBm/Hz, while receivers can operate with sensitivity levels equal to -72 dBm/Hz up to -77 dBm/Hz, with the reported capability of working within a threshold of -22 dB. The reference level of -22 dB is valuable to understanding the limitations of the PLC channel and will be used as the limit of attenuation between two modems.

V. FIELD TEST RESULTS AND ANALYSIS

This section delves into the specificity of the applied experiments that assessed the performance of the Setup. The results were obtained through three field experiments to assess the Setup performance under real-world conditions. The field experiments were carried out using the Setup illustrated in Fig. 6. Table V provides a comprehensive overview of the interconnections among the different Setups, delineating the connections and configurations implemented in each Setup. In all field experiments, the PLC coupling circuits were connected to the ends of the single-phase electric power line operating at 127 Vrms and 60 Hz, as shown in Fig. 6. The power cables consist of the concatenation of both PLC coupling circuits, where the DUT is the power cable modeled as a two-port network. Consequently, the measured scattering parameters corresponded to the circuit existing between the two PLC coupling circuits. The field experiments are described as follows:

- Field Experiment #1: Aimed to analyze the magnitude of the S_{21} scattering parameters and VSWR, providing insights into signal transmission over the DUT. Measurements of the magnitude S_{21} scattering parameters assessed the attenuation and power transfer characteristics, while VSWR measurements evaluated TL impedance matching compared to the modem power threshold for determining available bandwidth. As post-experiment, the PLC system bandwidth performance range will be evaluated for reliable signal transmission, which is pivotal for understanding operational limitations and capabilities.

- Field experiment #2: This experiment focused on impedance measurements to gain valuable insights into the characteristics of the electric power line. Understanding the impedance is essential

for designing and optimizing PLC coupling circuits to ensure maximum power transfer, minimize signal reflection, and reduce signal loss.

TABLE V. SETUP OF FIELD EXPERIMENTS.

Setup	Derivation in point A	Derivation in point B
#1	without	without
#2	2 m	without
#3	without	3 m
#4	2 m	3 m

A. Field experiment #1: the magnitude S_{21} scattering parameters and VSWR

In PLC systems, the magnitude S_{21} scattering parameters depict signal attenuation within electric power lines, impacting communication quality due to factors including impedance mismatches and signal attenuation. Another critical PLC parameter is VSWR, gauging transmission efficiency and impedance matching. High VSWR values signify poor match, causing power reflections and possible signal loss. These measurements offer insights to enhance PLC performance and ensure reliability. The cases elucidated in the results Setups 1 up to 4 in the subsequent subsections encompass the three distinct scenarios of establishing connections between P-N, P-PE, and N-PE lines.

1) Setup 1 analysis without branch:

Fig. 9(a) displays the magnitude S_{21} scattering parameter, depicting the modem's detection threshold at -22 dB by the dashed line. In Case 1, spanning the frequency range of 2-65 MHz, the magnitude of the S_{21} scattering parameter demonstrates that modem communication remains within the prescribed threshold of -22 dB. In Cases 2, 3, 4, 6, 7, 8, and 9, the analysis reveals notches of attenuation below the modem's detection threshold of -22 dB, indicating that at various frequencies, the PLC modem signal will not be detected. Notably, in Case 3, the threshold of -22 dB surpasses the limit above 55 MHz, and a notable instance of significant communication degradation is noted. In Case 5, the modem signal detection threshold is available from 2-40 MHz, 42-52 MHz, and 56-70 MHz. Between 67 MHz and 100 MHz, the magnitude of the S_{21} scattering parameter of all cases is predominantly below the modem signal detection threshold, except for Cases 1, 2, 4, and 5, which have minor frequency bands above the PLC modem detection threshold of -22 dB. Finally, Case 9 exhibits complete availability up to 40 MHz, and Cases 7 and 8 show notable attenuation in the magnitude of the S_{21} scattering parameter at 70 MHz and 98 MHz.

The VSWR analysis, in the Fig. 9(b), reveals marginal discrepancies at peak levels with impact on performance, attributed to their high values indicating significant impedance mismatch. Frequencies below 25 MHz exhibit pronounced impedance mismatch, evidenced by multiple peaks VSWR values across some Cases, reaching 6.2 in Case 3. Between 25-100 MHz, VSWR curves exhibit different behavior across all Cases, reaching a maximum value of 5.6 at 45 MHz for Case 4. The exceptionally high VSWR values indicate significant impedance mismatch across most frequency bands, particularly between 38-63 MHz and 70-100 MHz, suggesting substantial signal reflection. This impedance mismatch in the entire frequency spectrum underscores the necessity for optimizing signal transmission and mitigating signal loss.
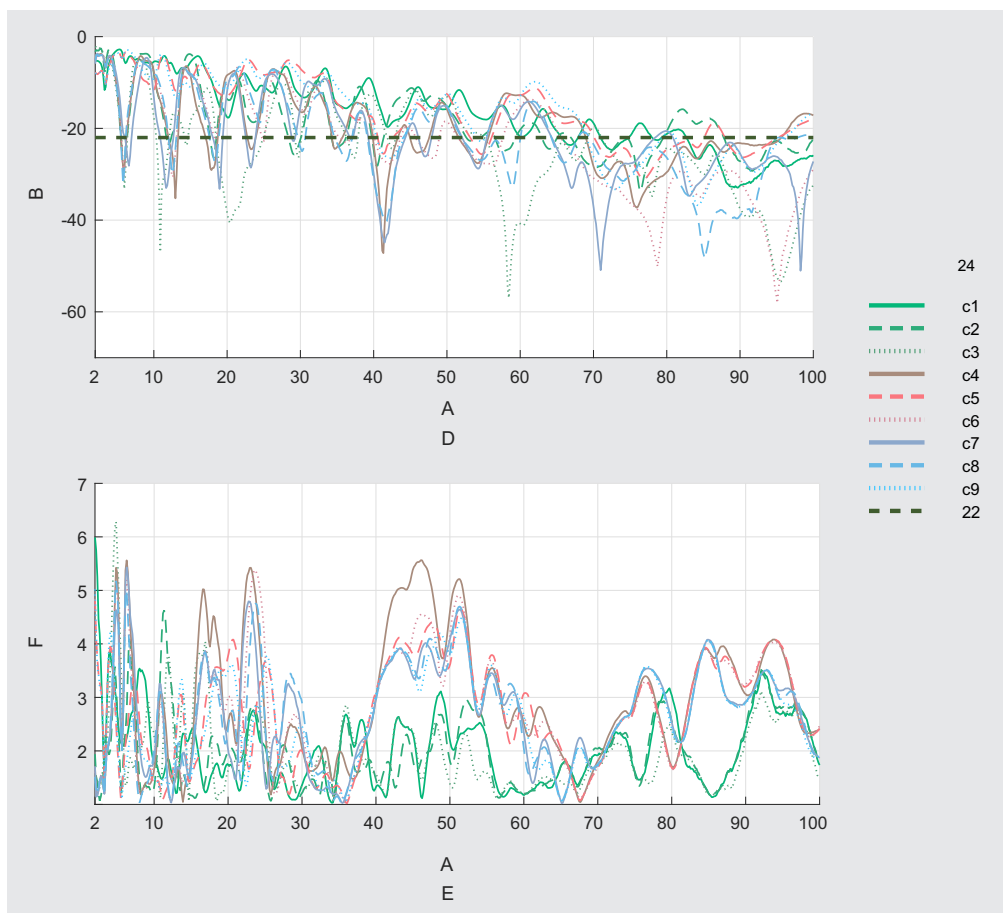
Fig. 9. The measurements results for Setup 1 without branch.

2) Setup analysis with a 2 m of branch:

In Fig. 10(a), within the frequency range of 2-19 MHz, in Cases 1 and 5, communication between PLC modems is feasible above the detection threshold of -22 dB. Case 1, which exhibits a broader frequency band conducive to communication considering the detection threshold of -22 dB, communication between PLC modems is also available between 58-100 MHz. Beyond 58 MHz up to 100 MHz, the channel's attenuation typically exceeds the -22 dB threshold in practically all cases. Notice that after introducing a 2 m electrical outlet, a notch is evident, with attenuation values of the magnitude S_{21} scattering parameters ranging between -29 dB and -58 dB, observed between 18-22 MHz, below the detection threshold of -22 dB of the PLC modem. For Cases 4 and 6, communication becomes unattainable below the -22 dB threshold after 65 MHz. Analyzing Fig. 10(a), communication with PLC modems remains available for Case 9 within the 2-20 MHz and 22-82 MHz frequency ranges. Cases 7 and 8 render modem communication unfeasible at frequencies below the -22 dB threshold, with Case 8 exhibiting a notable 50 dB attenuation at 19 MHz.

Fig. 10(b), between 2-30 MHz and 40-60 MHz, high VSWR values are observed, indicating a significant impedance mismatch, reaching a maximum value of 6.3 at 4 MHz. This mismatch between the impedance of the TL and the PLC modem can result in inefficient power transfer, signal reflection, and increased attenuation of the transmitted signal degrading the performance of the communication network. Some points on the curve in Fig. 10(b) show good impedance matching, such as 29 MHz for

Brazilian Microwave and Optoelectronics Society-SBMO   received 28 Oct 2023; for review 23 Nov 2023; accepted 23 Apr 2024

Brazilian Society of Electromagnetism-SBMag   © 2024 SBMO/SBMag   (cc) BY   *ISSN 2179-1074*

Case 4, 36 MHz for Cases 5 up to 7, and 67 MHz for Cases 6 and 7. The insertion of a 2 m branch did not significantly alter the VSWR curve in Fig. 10(b) compared to Fig. 9(b).
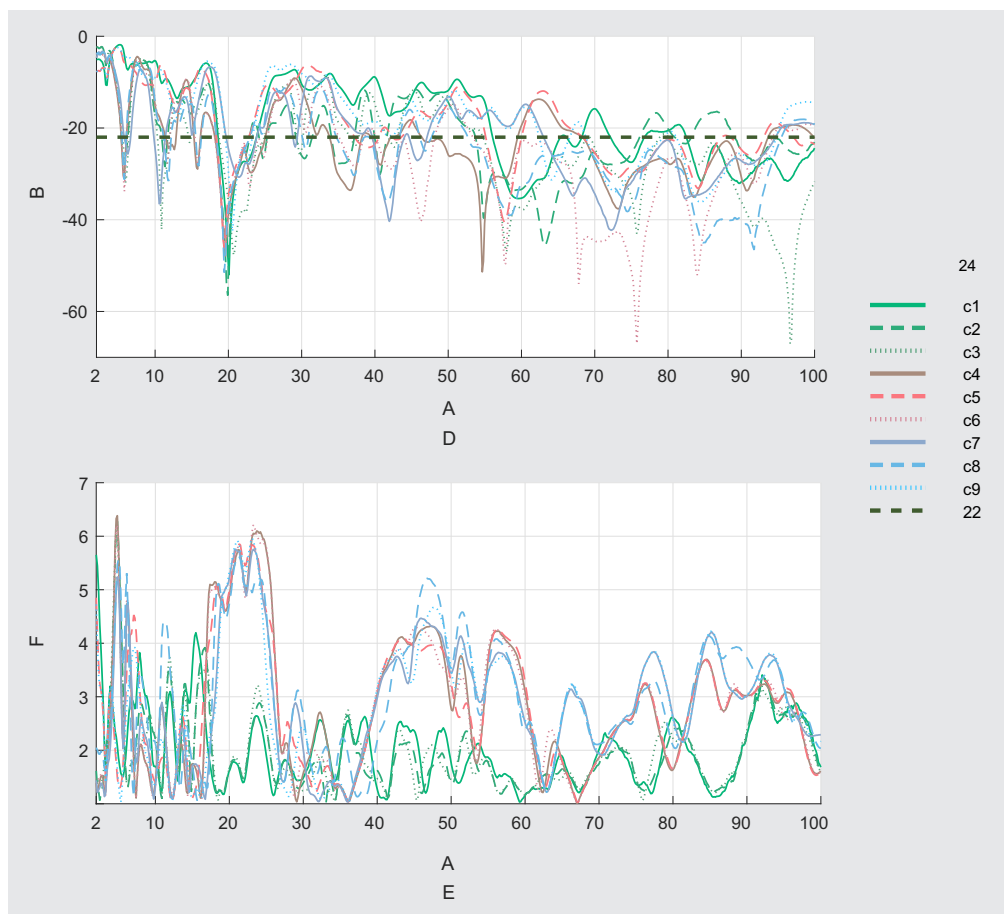

Fig. 10. The measurements results for Setup 2 with 2 m of branch.

3) Setup 3 analysis with a 3 m branching:

In the analysis of Fig. 11(a), the severity of signal degradation in PLC modems is evaluated by comparing the curves with the limit threshold of -22 dB, revealing a lack of communication for the PLC between 12-14 MHz, 42-43 MHz and 65-75 MHz for all cases. For Case 1, acceptable signal loss for the PLC modem is indicated between 2-12 MHz, 15-41 MHz, 43-65 MHz, and 75-82 MHz. In Cases 2 and 3, communication bands align with Case 1 up to 62 MHz. Note that with the insertion of a 3 m long outlet, two notches below -22 dB emerge where the PLC modem signal cannot be detected. One notch appears between 11-13 MHz, and the other is between 42-44 MHz.

Cases 7, 8, and 9 reveal close similarities with Fig. 10(a), and between 76-100 MHz Case 5, showed availability and more bandwidth in comparison with all Cases. Beyond 50 MHz, communication availability varies among the three Cases, and after 65 MHz, modem communication is restricted to Case 7 between 85-90 MHz and 96-100 MHz, while for Case 8, communication is feasible between 94-100 MHz.

In the analysis of VSWR curves shown in Fig. 11(b), there are some points of high values of impedance mismatch in comparison with Fig. 9(b) and Fig. 10(b). Notably, in the frequency band of 2-18 MHz, impedance mismatch peaks reached 7.8, indicating the presence of standing waves and

potential signal degradation. Between 18-85 MHz, the impedance mismatch values achieved maximum peaks of 13.9, demonstrating a high level of signal reflection. Beyond 85 MHz, the VSWR values continued to exhibit noteworthy impedance mismatch, with peaks reaching values greater than 14. Furthermore, it is noteworthy that within the frequency range of 30-40 MHz and 75-85 MHz, the VSWR values consistently demonstrate better characteristics, registering below 2.
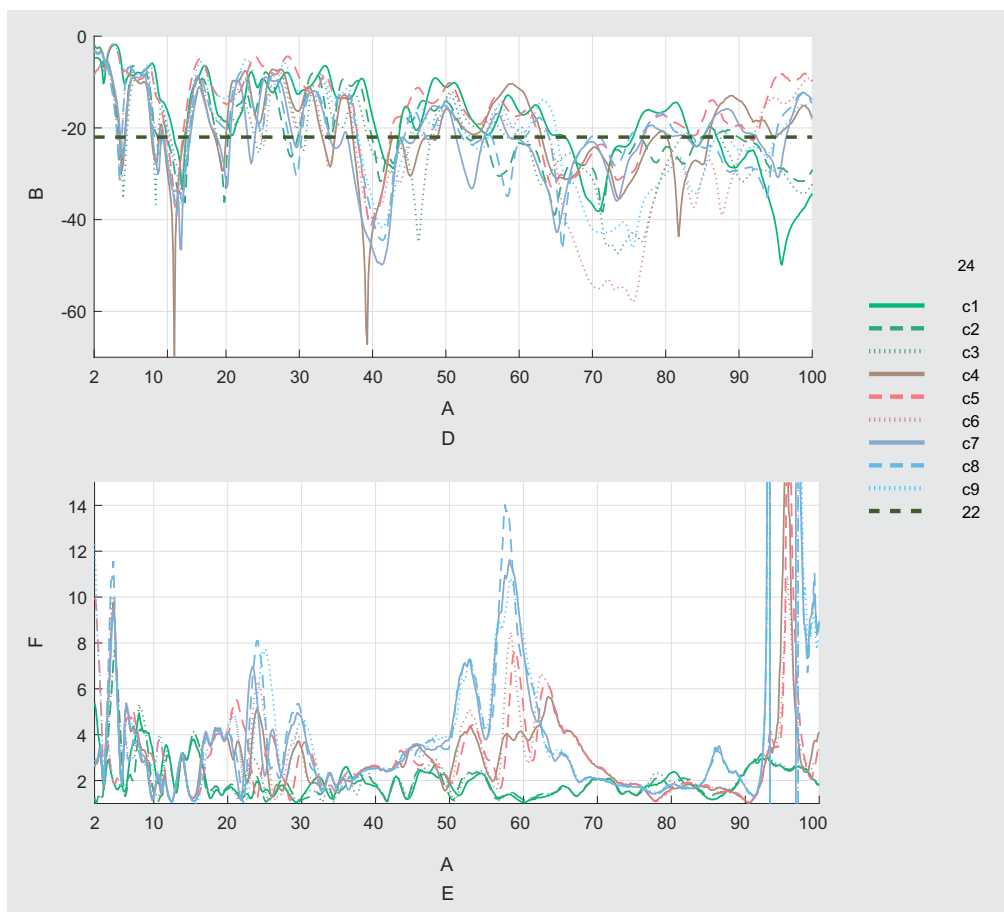

Fig. 11. The measurements results for Setup 3 with a 3 m of branch.

4) Setup 4 analysis with a 2 and 3 m branching:

In delving into the dynamics of PLC system, the depicted Fig. 12(a) unveils of signal transmission behavior through the magnitude of the S_{21} scattering parameter. Notice that with two branches added in this Setup test, the number of notches increases in comparison with the Setups 1 up to 3, and the availability of bandwidth decreases considering the threshold value of -22 dB.

Fig. 12(a) shows the same communication bandwidth availability for the Cases 2 and 4, 6 and 8 up to 55 MHz. The Cases 1, 5, and 9 have the same behavior up to 55 MHz. Between 85-100 MHz, communication is available for the PLC modem in Cases 5 and 6. Cases 1, 5 and 9 presents the same availability in the frequency range of 1-75 MHz.

Analysing Fig. 12(a), Case 9 distinguishes itself by boasting an ample bandwidth availability, mainly in the frequency range of 25-55 MHz. It presents exciting prospects for high-speed data transmission and efficient communication within this frequency band.

The VSWR analysis highlights distinct impedance mismatch patterns across different frequency

ranges. Particularly, the frequency span of 2-30 MHz exhibits impedance mismatching for Cases 2, 4, 6, and 9, in which VSWR values fluctuate within the range of 11 and 9.3. Except for Case 1, all other Cases exhibit high impedance mismatch between 20-27 MHz, 55-65 MHz, and 93-100 MHz. Remarkably, a striking similarity is observed between the VSWR curve in this Setup and those shown in Fig. 11(b). Additionally, Case 1 presents the best impedance matching when compared to the other Cases.
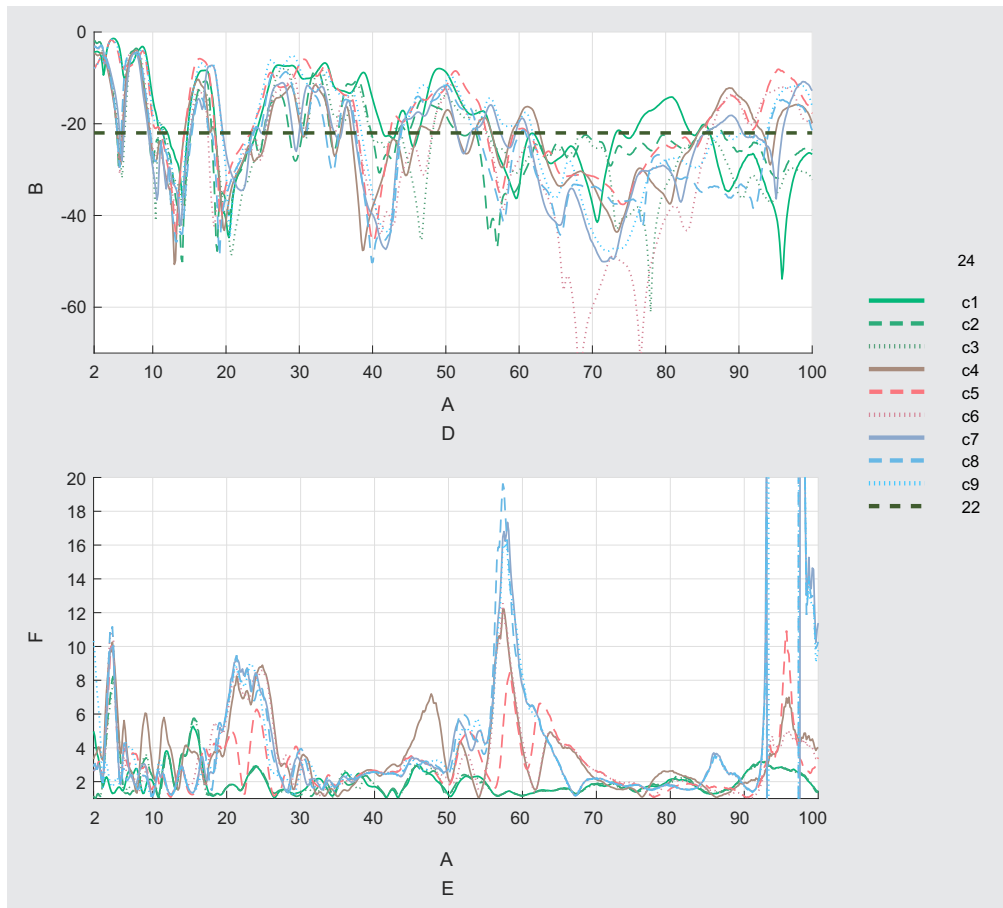

Fig. 12. The measurements results for Setup 4 with branches of 2 and 3 m.

5) Bandwidth Availability:

To compare all the Setups analyzed in the previous subsections, Table VI gathers all the data addressed by the Setups and Cases based on the availability of bandwidth. Bandwidth availability, a critical metric in telecommunications engineering, is essential for assessing the capacity and efficiency of communication channels. This study systematically performs comprehensive bandwidth measurements across the frequency spectrum ranging from 2-100 MHz, focusing on regions where the S_{21} scattering parameter exceeds the critical threshold of -22 dB. Subsequently, the cumulative bandwidths corresponding to these identified regions are aggregated to yield the comprehensive assessment of total available bandwidth as illustrated in Table VI.

Regarding MIMO channels, Case 1 presents the highest bandwidth availability in Setup 1 (74.64%), which signifies a potential advantage in supporting multiple data streams simultaneously. This scenario suggests that Case 1 network configuration may effectively utilize spatial diversity and multiplexing

TABLE VI. BANDWIDTH AVAILABILITY.

Case	Setup 1 (%)	Setup 2 (%)	Setup 3 (%)	Setup 4 (%)
Case 1	74.64	60.42	70.92	54.12
Case 2	59.61	49.43	46.53	34.41
Case 3	42.81	42.97	47.98	34.57
Case 4	55.74	42.97	60.10	47.01
Case 5	72.05	59.13	77.54	59.29
Case 6	47.82	36.67	54.28	43.94
Case 7	49.27	53.31	50.57	46.69
Case 8	48.14	38.61	56.38	39.26
Case 9	69.63	67.04	59.13	54.09

techniques inherent in MIMO systems. Similarly, Case 5 shows superior bandwidth availability in Setup 3 (77.54%), indicating a capacity for data transmission, which could be further enhanced in MIMO environments through spatial multiplexing and diversity gains.

Conversely, the lowest bandwidth availability in Setup 4 for Case 1 (54.12%) and Case 2 (34.41%) suggests potential challenges in maintaining reliable communication channels, especially in MIMO channels. Low bandwidth availability can intensify channel fading, multipath interference, and signal degradation, impacting the overall data rate quality.

The discrepancy between direct and cross-wire channels underscores the importance of accounting for channel characteristics and network configurations when evaluating bandwidth availability in MIMO systems. By addressing challenges associated with cross-wire channels, such as mitigating interference, and implementing advanced signal processing techniques, overall network performance and communication reliability can be enhanced.

Integrating MIMO channels provides valuable insights into the interaction between network configurations, channel characteristics, and bandwidth availability. By acknowledging the differences between direct and cross-wire channels and implementing strategies to mitigate associated challenges, the full potential of MIMO technology contributes to optimizing data transmission and guaranteeing communication in several scenarios.

6) General Comments the Magnitude of the S_{21} Scattering Parameter Analysis and VSWR:

The comprehensive analysis of PLC systems relies on the magnitude of the S_{21} scattering parameters, meticulously quantifying signal transmission behavior across different ports (P, N, and PE). The absence of branches not only simplifies but also streamlines the analytical process, facilitating an unambiguous interpretation of S-parameters. For the impact of introducing branches into the PLC system, additional experiments were conducted where branches were integrated into the electric power line. Note that the introduction of branches at 2 m and 3 m resulted in two deep notches for all Cases at 20 MHz in the analysis of Setup 2 and 4, and at 12 MHz for Setup 3 and 4 in comparison with the Setup 1. After 50 MHz, the curves for Setups 1 and 2 become similar, and the same analysis can be done for Setups 3 and 4. These experiments reveal a notable degradation in the magnitude of the S_{21} scattering parameters, indicating worsening signal transmission characteristics. As more branches are introduced, the spreading parameters exhibit a consistent deterioration, and the availability of the -22 dB limit diminishes progressively. Consequently, the PLC communication bandwidth experiences a significant reduction with each added branch. In networks without branches, there are fewer components causing

signal loss and impedance mismatches, resulting in a more direct path for the signal with reduced attenuation. Overall, in electric power lines without branches, the improved signal integrity leads to a more robust and dependable communication system.

The inclusion of branches into a PLC system introduces impedance mismatches, causing signal reflections and elevating VSWR. These reflections induce standing waves that impact the magnitude of the S_{21} scattering parameter, representing signal transmission between ports. The addition of branches results in heightened signal loss as a consequence of extra components and wiring, contributing to diminished effectiveness of the magnitude S_{21} scattering parameter.

The variability in impedance conditions, introduced by the branches, leads to unpredictable changes in transmission properties due to differing impedance. Comparing VSWR curves with those in a similar Setup, we found striking similarities in impedance mismatch patterns for Cases 1 up to 3, Cases 4 up to 6, Cases 7 and 8, highlighting the reproducibility of impedance mismatch characteristics. Notice that, in all VSWR Setups analyzed, the Cases 1 up to 3 achieved the best impedance matching where the connection corresponding wires with similar functions on both sides of the electric power line. In Case 1 (P1N1-P2N2), the phase (P) and neutral (N) wires are connected on both sides. The protective earth introduces additional grounding effects that can affect the impedance of the TLs and associated components. Cases 7, 8, and 9 present high values of impedance mismatch after $50 \, \text{MHz}$ for Setups 2 up to 4, and in the Setup 1, the values have the behavior similar to other Cases. The complex network structure resulting from branch introduction poses challenges in maintaining uniform impedance and signal characteristics, making optimization of the system for efficient signal transmission more intricate.

B. Field experiment #2: Impedance Analysis

The analysis of the electric power line impedance is essential for understanding the dynamics of PLC networks. This subsection explores the various factors affecting impedance, including cable characteristics, branch configurations, and frequency effects, providing critical insights into the impedance analysis and its significance for optimizing PLC network performance.

1) Factors Influencing Electric Power Line Impedance:

The input impedance of the electric power line significantly impacts the performance and reliability of PLC networks. The power line's impedance directly influences the signal attenuation which is one of the key factors affecting the overall data transmission quality. Therefore, accurate measurement and analysis of the electric power line input impedance in the context of PLC are important for optimizing communication performance, ensuring seamless data transfer, and ultimately enabling the successful design of PLC coupling circuits.

In this context, some comparative analyses can be conducted between the VSWR curves obtained in Section V and the impedance measurement curves from this section. If we compare the VSWR curves in Fig. 9(b) with the curve in Fig. 13, we observe that the high VSWR values correspond to a higher impedance value in Fig. 13. Note that in Fig. 13, cases 4, 5, and 6 have impedance values very close to cases 7, 8, and 9. Furthermore, Cases 1, 2, and 3 exhibit some higher impedance values up to $15 \, \text{MHz}$, while for $20\text{-}100 \, \text{MHz}$, Cases 4 up to 9 present higher impedance values. This pattern is evident across Figs. 14, 15, and 16. Despite that, it is imperative to highlight significant findings when comparing the datasets from all four experimental setups. A noteworthy similarity is observed in impedance values

between measurements conducted without branching, as depicted in Fig. 9, and the insertion of the 2 m branch, as illustrated in Fig. 10. Analyzing the results of the four Setups, it is evident that Cases 1, 2, and 3 exhibit closely aligned impedance values. The impedance values increase with the insertion of a 3 m branch in Setups 3 and 4, from Cases 4 to 9, reaching values up to 700 Ω, as depicted in Fig. 16.

These findings are reflected in the impedance values observed in Table VII, which illustrates that measurements from Cases 4, 5, and 6 closely align with those from Cases 7, 8, and 9. Notably, across all setups, Cases 1 up to 3 consistently exhibit very similar impedance values. Conversely, for Cases 4 up to 9, there is an increase in impedance as the number of branches in the circuit rises. Setups 1 and 2 demonstrate nearly identical impedance values for Cases 1 up to 9, while Setups 3 and 4 follow a similar pattern, with impedance values closely clustered. An additional significant observation is the progressive increase in impedance with the augmentation of branch numbers in the circuit.

The length and configuration of the TLs, the characteristics of the cables used, and the presence of branches cause reflections and change the characteristics of the electric power line. At lower frequencies, the impedance may be influenced by the distributed capacitance and inductance of the TLs, and any distributed resistive losses. When branches are introduced into the electric power line, the impedance values between 20-100 MHz can be higher. The introduction of branches alters the overall impedance characteristics of the electric power line, causing changes in signal propagation, reflections, and impedance matching. Additionally, at higher frequencies, factors such as skin effect and dielectric losses may also play a role in influencing impedance values.

2) General Comments Impedance Analysis:

The input impedance of in-home electric power lines typically depends on various factors, including the type of wiring, its length, the number of branches for outlets, and appliances connected to the electric power line. In power line cables, the input impedance exhibits frequency-dependent behavior due to the distributed nature of electric power lines and the associated parameters. Unlikely coaxial and twisted-pair cables, where impedance tends to be relatively constant with increasing frequency, power line cables are subject to unique challenges and variations that contribute to their frequency-dependent characteristics. High-frequency signals experience skin effects and proximity effects. The skin effect causes the current to concentrate near the surface of the conductor, impacting the effective resistance (R). The proximity effect, which is more pronounced at higher frequencies, affects the effective inductance (L). Electric power lines are surrounded by insulation materials with frequency-dependent dielectric properties. The distributed capacitance (C) is influenced by the dielectric constant of the surrounding material, and this dependency on frequency affects the overall impedance. Electric power line cables exhibit frequency-dependent losses, with factors such as dielectric and conductor losses becoming more pronounced at higher frequencies. These losses lead to changes in impedance across all frequency bands.

In this paper, the measured impedance of various Cases and Setups have been analyzed to gain insights into their behavior. The mean impedance for each Case and Setup has been calculated from the scattering parameters measured by a VNA and shown in Table VII. The overall average impedance found is 77.14 Ω, which is remarkably close to the 50 Ω impedance of the VNA. The mean impedance values hold significance, particularly in the context of PLC coupling circuit design, serving as an approximation aimed at achieving the best impedance matching between PLC coupling circuits and the electric power line.
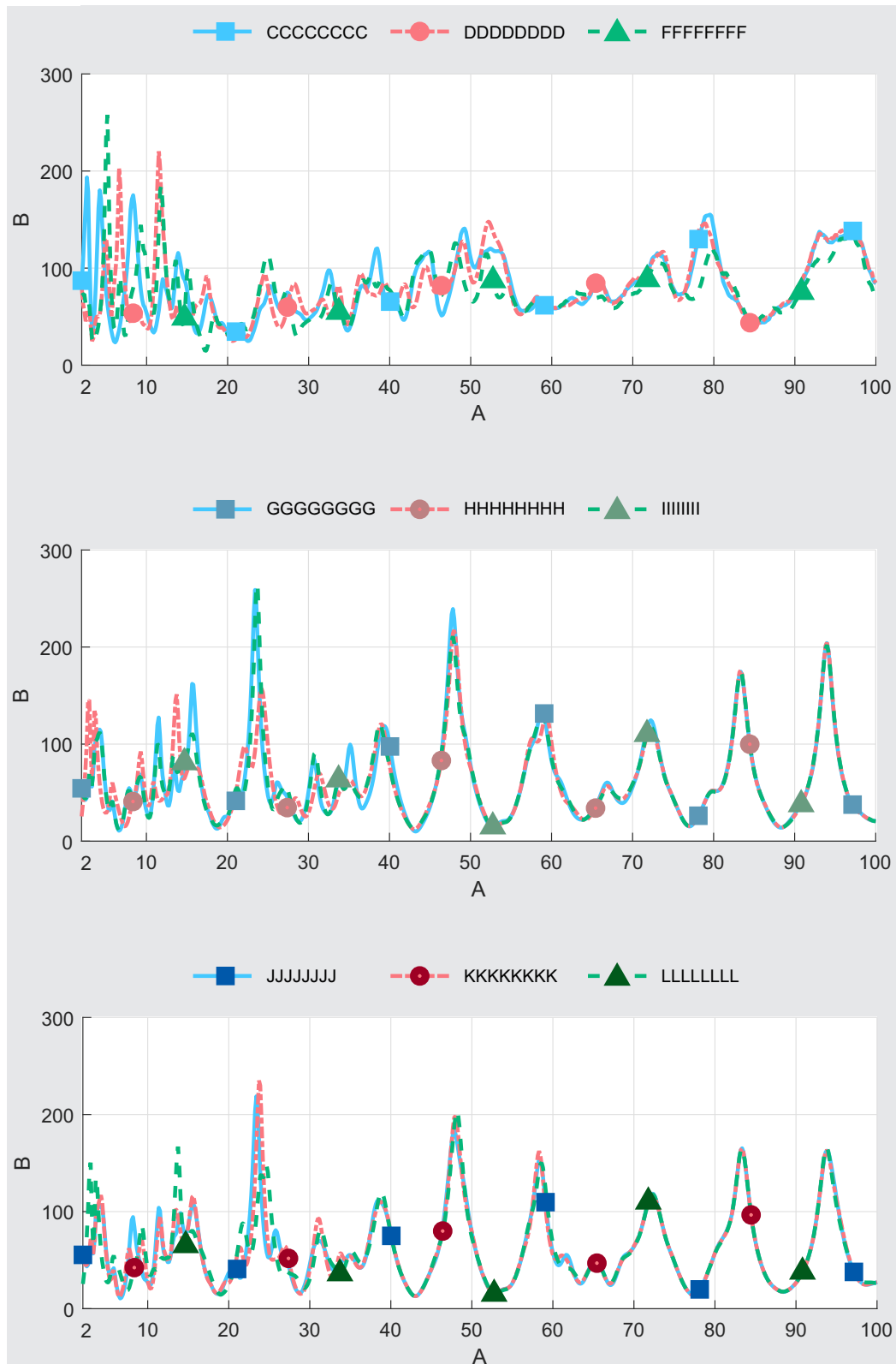
Fig. 13. Electric Power Line Impedance Profile for Setup 1.

The electric power line's characteristics, including length, topology, and cable types, exhibit significant variations across different environments. These disparities can yield diverse impedances along the line, posing challenges in achieving precise impedance matching between transmitting and receiving
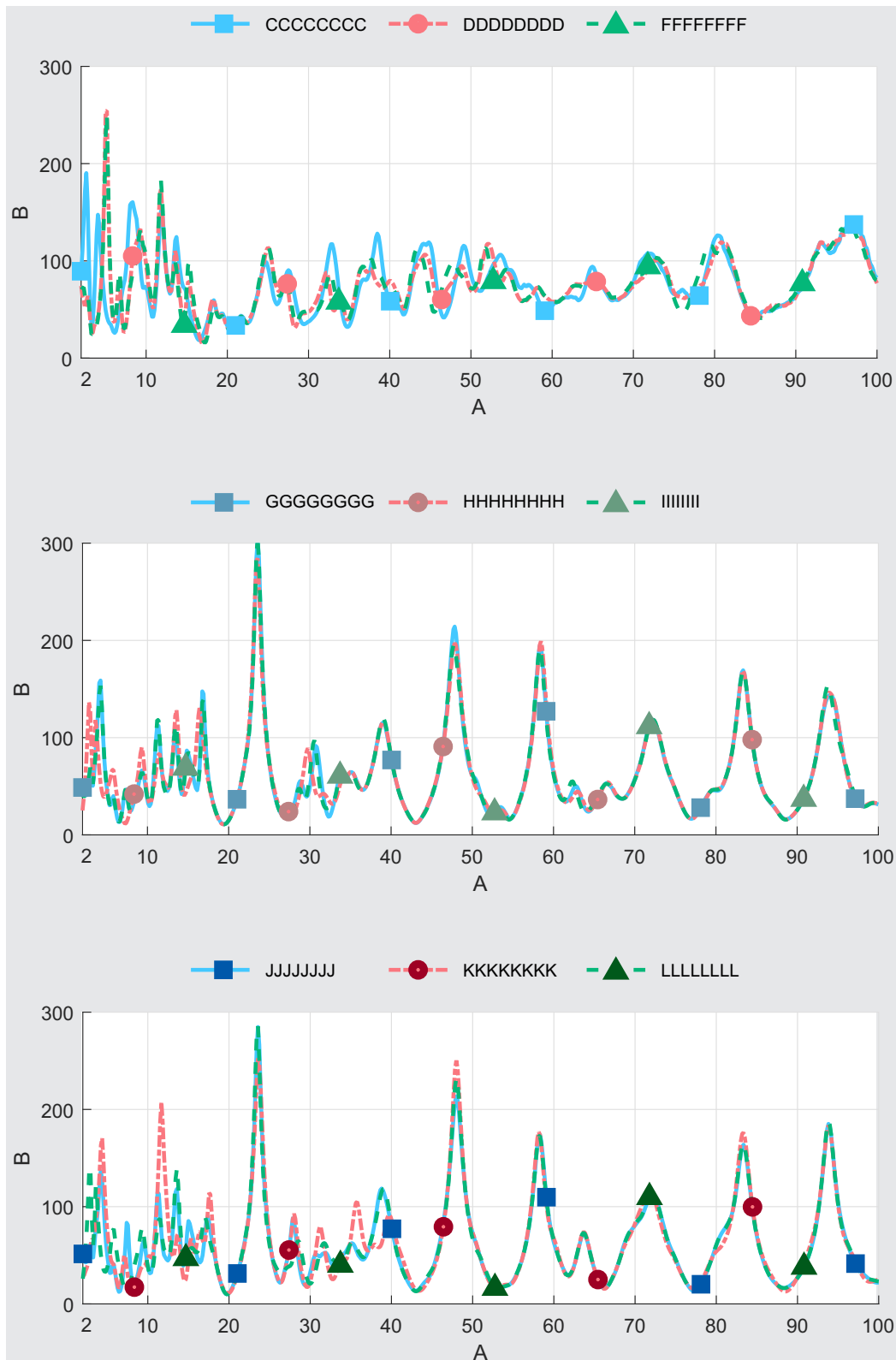
Fig. 14. Electric Power Line Impedance Profile for Setup 2.

devices. To address these issues, signal processing techniques such as amplification, equalization, and adaptive filtering are commonly employed in PLC coupling circuits [42], [43]. These methods effectively compensate for impedance variations and alleviate the repercussions of impedance mismatching, con-
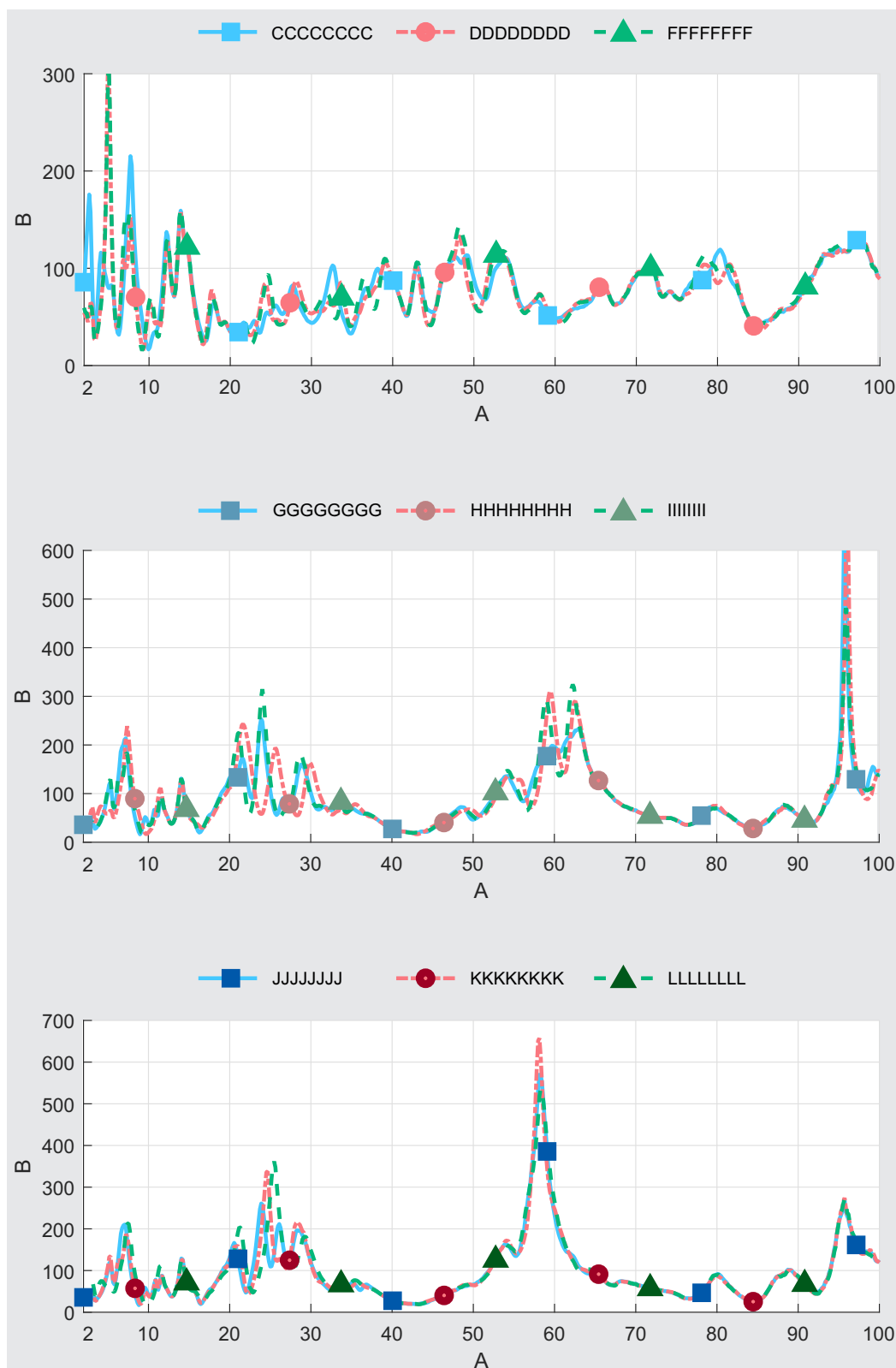
Fig. 15. Electric Power Line Impedance Profile for Setup 3.

sequently enhancing the availability of the S_{21} scattering parameter. Designing PLC coupling circuits with an impedance value matching the average impedance of $77.14\,\Omega$ presents a viable solution to overcome impedance matching challenges in electric power line communication systems.
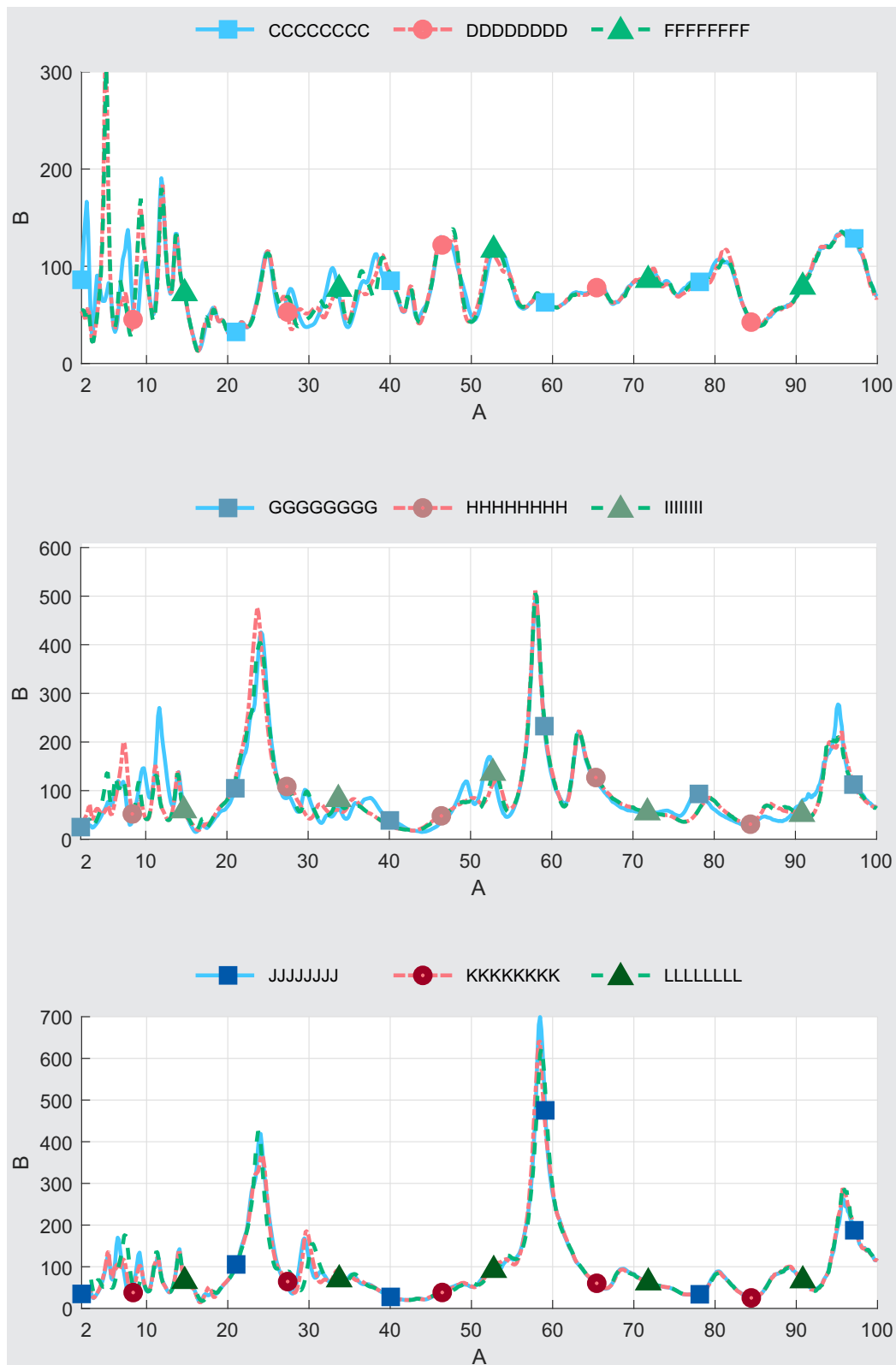
Fig. 16. Electric Power Line Impedance Profile for Setup 4.

The measurements discussed in this work can be seen as multiple measurements varying across measurement setups, interleaving between phase, neutral, and protective earth. A stochastic process achieves stability when its probability distribution remains unchanged regardless of shifts in time.

TABLE VII. AVERAGE IMPEDANCE OF ELECTRIC POWER LINE.

Case	Setup 1 (Ω)	Setup 2 (Ω)	Setup 3 (Ω)	Setup 4 (Ω)
Case 1	80.47	76.75	76.47	76.62
Case 2	79.77	75.52	75.82	76.74
Case 3	75.94	75.76	76.87	76.66
Case 4	62.39	62.11	87.36	92.54
Case 5	61.11	61.99	88.84	91.28
Case 6	61.61	61.90	88.18	89.89
Case 7	60.81	62.12	96.06	95.43
Case 8	60.87	63.43	96.49	94.99
Case 9	60.76	62.35	97.08	94.23

Essentially, if we observe the measurements at a specific time, the values will maintain consistency when observed at any other time. While individual elements within the measurements may vary over time, changes in one element correspond to others reverting to previous values. Therefore, determining the exact moment of measurement becomes challenging.

VI. CONCLUSION

This paper is focused on analyzing the scattering parameters, VSWR, and input impedance of the energized electrical power line, considering four test setups. The deterministic modeling approach was used, assuming the behavior of the electric power line is free from randomness. The results revealed that certain frequency ranges provided acceptable communication performance for PLC modems, while others exhibited significant attenuation and impedance mismatch, making communication infeasible.

The discrepancy observed between direct and cross-wire channels underscores the importance of factoring in channel attributes and network setups when evaluating bandwidth availability in MIMO systems. Strategies aimed at addressing challenges associated with cross-wire channels, such as interference mitigation and the adoption of advanced signal processing techniques, have the potential to enhance network performance and fortify communication reliability.

The impedance analysis revealed significant variations in the electric power line impedance at different frequencies, impacting signal attenuation, noise propagation, and overall data transmission quality. This study provides valuable insights into the performance of PLC systems, identifying optimal Setups for communication and emphasizing the importance of impedance measurements for optimizing signal transmission and system stability in PLC networks. Further research and optimization efforts can build upon these findings to enhance the reliability and efficiency of PLC communication systems in real-world scenarios.

VII. FUTURE WORK

As a future work, it is proposed to redo the study by incorporating different loads and conducting measurements of scattering parameters, VSWR, and impedance. By varying the loads connected to the electric power line, a more thorough understanding of the system's behavior and performance can be gained. This expanded investigation will provide valuable insights into how different loads affect signal propagation, attenuation, and impedance matching. Additionally, conducting a detailed analysis of the effects of diverse loads on the system's behavior will contribute to the optimization of PLC coupling circuits and enhance the overall efficiency and reliability of PLC.

REFERENCES

[1] G. J. Foschini and M. J. Gans, "On limits of wireless communications in a fading environment when using multiple antennas," *Wireless personal communications*, vol. 6, pp. 311–335, 1998, doi: 10.1023/A:1008889222784.

[2] L. Yonge, J. Abad, K. Afkhamie, L. Guerrieri, S. Katar, H. Lioe, P. Pagani, R. Riva, D. M. Schneider, and A. Schwager, "An overview of the homeplug AV2 technology," *Journal of Electrical and Computer Engineering*, vol. 2013, pp. 1–21, 2013, doi: 10.1155/2013/892628.

[3] L. G. da S. Costa, G. R. Colen, A. C. M. de Queiroz, V. L. R. da Costa, U. R. C. Vitor, F. V. dos Santos, and M. V. Ribeiro, "Access impedance in Brazilian in-home, broadband and low-voltage electric power grids," *Electric power systems research*, vol. 171, pp. 141–149, 2019, doi: 10.1016/j.epsr.2019.02.015.

[4] K. Rabie, A. M. Tonello, N. Al-Dhahir, J. Song, and A. Sendin, "IEEE access special section editorial: Advances in power line communication and its applications," *IEEE Access*, vol. 7, pp. 133 371–133 374, 2019, doi: 10.1109/AC-CESS.2019.2942516.

[5] B. Barakat, A. Taha, R. Samson, A. Steponenaite, S. Ansari, P. M. Langdon, I. J. Wassell, Q. H. Abbasi, M. A. Imran, and S. Keates, "6G opportunities arising from internet of things use cases: A review paper," *Future Internet*, vol. 13, no. 6, 2021, doi: 10.3390/fi13060159.

[6] C. Nieß and G. Bumiller, "Impedance measurement system for actively transmitting loads on power line," in *Proc. IEEE International Symposium on Power Line Communications and its Applications*, pp. 1–5, 2020, doi: 10.1109/ISPLC48789.2020.9115389.

[7] S. S. Dash and A. V. Panda, "Interpretation of different channel configurations and modulation techniques over power line communication," in *Proc. International Conference on Communication and Signal Processing*, pp. 420–425, 2016, doi: 10.1109/ICCSP.2016.7754170.

[8] U. R. C. Vitor, M. C. de Sousa, D. A. B. Fonseca, L. R. G. S. L. Novo, M. T. de Melo, M. E. V. Segatto, and G. G. Machado, "MIMO-PLC communications in an experimental medium voltage network: Measurement and analysis," *Journal of Microwaves, Optoelectronics and Electromagnetic Applications*, vol. 21, pp. 102–113, 2022, doi: 10.1590/2179-10742022v21i11380.

[9] A. Schwager, D. Schneider, W. Bäschlin, A. Dilly, and J. Speidel, "MIMO PLC: Theory, measurements and system setup," in *Proc. IEEE International Symposium on Power Line Communications and Its Applications*, pp. 48–53, 2011, doi: 10.1109/ISPLC.2011.5764447.

[10] M. Tanaka, "High frequency noise power spectrum, impedance and transmission loss of power line in Japan on intrabuilding power line communications," *IEEE Transactions on Consumer Electronics*, vol. 34, no. 2, pp. 321–326, 1988, doi: 10.1109/30.2948.

[11] E. K. Saathoff, S. R. Shaw, and S. B. Leeb, "Line impedance estimation," *IEEE Transactions on Instrumentation and Measurement*, vol. 70, pp. 1–10, 2021, doi: 10.1109/TIM.2020.3039642.

[12] M. Antoniali and A. M. Tonello, "Measurement and characterization of load impedances in home power line grids," *IEEE Transactions on Instrumentation and Measurement*, vol. 63, no. 3, pp. 548–556, 2014, doi: 10.1109/TIM.2013.2280490.

[13] G. Artale, G. Caravello, A. Cataliotti, V. Cosentino, D. Di Cara, R. Fiorelli, S. Guaiana, N. Panzavecchia, and G. Tinè, "A line impedance calculator based on a G3 PLC modem platform," *IEEE Transactions on Instrumentation and Measurement*, vol. 71, pp. 1–10, 2022, doi: 10.1109/TIM.2022.3146629.

[14] M. A. O. Kharraz, P. Jensen, V. Audebert, A. Jeandin, C. Lavenu, D. Picard, and M. Serhir, "Experimental characterization of outdoor low voltage cables for narrowband power line communication," in *Proc. International Symposium on Power Line Communications and its Applications*, pp. 138–143, 2016, doi: 10.1109/ISPLC.2016.7476267.

[15] S. Moaveninejad, A. Saad, and M. Magarini, "Enhancing the performance of WiNPLC smart grid communication with MIMO NB-PLC," in *Proc. IEEE International Conference on Environment and Electrical Engineering and IEEE Industrial and Commercial Power Systems Europe*, pp. 1–6, 2017, doi: 10.1109/EEEIC.2017.7977639.

[16] "IEEE standard for broadband over power line networks: Medium access control and physical layer specifications," *IEEE Std 1901-2020 (Revision of IEEE Std 1901-2010)*, pp. 1–1622, 2021, doi: 10.1109/IEEESTD.2021.9329263.

[17] I. H. Cavdar and E. Karadeniz, "Measurements of impedance and attenuation at CENELEC bands for power line communications systems," *Sensors*, vol. 8, no. 12, pp. 8027–8036, 2008, doi: 10.3390/s8128027.

[18] J. Bausch, T. Kistner, M. Babic, and K. Dostert, "Characteristics of indoor power line channels in the frequency range 50-500 kHz," in *Proc. IEEE International Symposium on Power Line Communications and Its Applications*, pp. 86–91, 2006, doi: 10.1109/ISPLC.2006.247442.

[19] G. Hallak and G. Bumiller, "Impedance measurement of electrical equipment loads on the power line network," in *Proc. IEEE International Symposium on Power Line Communications and its Applications*, pp. 1–6, 2017, doi: 10.1109/ISPLC.2017.7897099.

[20] L. Callegaro, *Electrical Impedance: Principles, Measurement, and Applications*.   Boca Raton, USA: CRC Press, 2013.

[21] F. Passerini and A. M. Tonello, "Analysis of high-frequency impedance measurement techniques for power line network sensing," *IEEE Sensors Journal*, vol. 17, no. 23, pp. 7630–7640, 2017, doi: 10.1109/JSEN.2017.2732737.

[22] G. Hallak, C. Nieß, and G. Bumiller, "Accurate low access impedance measurements with separated load impedance measurements on the power-line network," *IEEE Transactions on Instrumentation and Measurement*, vol. 67, no. 10, pp. 2282–2293, 2018, doi: 10.1109/TIM.2018.2814138.

[23] D. M. Pozar, *Microwave Engineering*.   John Wiley & Sons, 2011.

[24] A. H. Halid Hrasnica and R. Lehnert, *Broadband Power Line Communication*.   San Francisco, USA: John Wiley & Sons, 2004.

[25] U. R. C. Victor, "Internet via rede elétrica: Modelagem de canal baseada em interferômetro," Dissertacao submetida ao Programa de Pós-Graduação em Engenharia Elétrica da Universidade Federal de Pernambuco. Recife PE, 2008.

[26] D. K. Cheng, *Field and Wave Electromagnetics*, 2nd ed.   New Jersey, USA: Prentice Hall, 1989.

[27] L. Wilson, *The Circuit Designer's Companion*.   Kidlington, UK: Newnes, 2017.

[28] J. González-Ramos, I. Angulo, A. Arrinda, I. Fernández, A. Gallarreta, D. de la Vega, A. Sendin, I. Berganza, R. Ayala, and J. S. Gómez, "Characterization of the LV distribution grid for the deployment of a pilot BB-PLC network," in *Proc. IEEE International Symposium on Power Line Communications and its Applications*, pp. 19–24, 2023, doi: 10.1109/ISPLC57122.2023.10104185.

[29] G. Artale, A. Cataliotti, V. Cosentino, S. Guaiana, D. Di Cara, N. Panzavecchia, G. Tinè, and R. Fiorelli, "An innovative coupling solution for power line communication in MV electrical networks," in *Proc. 1st Global Power, Energy and Communication Conference*, pp. 90–95, 2019, doi: 10.1109/GPECOM.2019.8778524.

[30] Y. Li, M. Zhang, W. Zhu, M. Cheng, C. Zhou, and Y. Wu, "Performance evaluation for medium voltage MIMO-OFDM power line communication system," *China Communications*, vol. 17, no. 1, pp. 151–162, 2020, doi: 10.23919/JCC.2020.01.012.

[31] D. Halliday, R. Resnick, and J. Walker, *Fundamentos de Física - Eletromagnetismo, vol. 3*.   Rio de Janeiro, Brazil: LTC, 2003.

[32] E. G. Bakhoum, "s-parameters model for data communications over 3-phase transmission lines," *IEEE Transactions on Smart Grid*, vol. 2, no. 4, pp. 615–623, 2011, doi: 10.1109/TSG.2011.2168613.

[33] L. T. Berger, A. Schwager, P. Pagani, and D. Schneider, *MIMO Power Line Communications*.   Boca Raton, USA: CRC Press, 2014.

[34] Rohde and Schwarz, "FSH8 Vector Network Analyzer 2 ports, 100 kHz - 8 GHz," https://www.testequipmenthq.com/datasheets/Rohde-Schwarz-FSH8-Datasheet.pdf, Jun. 2023.

[35] A. Rumiantsev and N. Ridler, "VNA calibration," *IEEE Microwave magazine*, vol. 9, no. 3, pp. 86–99, 2008.

[36] A. A. M. Picorone, T. R. de Oliveira, R. Sampaio-Neto, M. Khosravy, and M. V. Ribeiro, "Channel characterization of low voltage electric power distribution networks for PLC applications based on measurement campaign," *International Journal of Electrical Power & Energy Systems*, vol. 116, pp. 1–9, 2020, doi: 10.1016/j.ijepes.2019.105554.

[37] C. Zhang, X. Zhu, Y. Huang, and G. Liu, "High-resolution and low-complexity dynamic topology estimation for PLC networks assisted by impulsive noise source detection," *IET Communications*, vol. 10, no. 4, pp. 443–451, 2016, doi: 10.1049/iet-com.2015.0454.

[38] T. R. Oliveira, A. A. M. Picorone, C. B. Zeller, S. L. Netto, and M. V. Ribeiro, "Statistical modeling of brazilian in-home PLC channel features," *Journal of Communication and Information Systems*, vol. 34, no. 1, pp. 154–168, 2019, doi: 10.14209/jcis.2019.16.

[39] Coilcraft, "Wideband RF transformers," https://www.coilcraft.com/en-us/products/transformers/wideband-rf-transformers/, Jun. 2023.

[40] L. G. da S. Costa, A. A. M. Picorone, A. C. M. de Queiroz, V. L. R. da Costa, and M. V. Ribeiro, "Projeto e caracterização de acopladores para power line communications," *in Proc. XXXIII Simpósio Brasileiro de Telecomunicações*, vol. 1, no. 1, pp. 1–5, 2015, doi: 10.14209/sbrt.2015.7.

[41] Corinex Communications, "Low Voltage and High-Density Gateway," https://svn.wirelessleiden.nl/svn/projects/nodebouwdocumentatie/, Jun. 2023.

[42] L. G. da S. Costa, T. C. Rocha, G. H. G. Borges, W. M. Cantarino, G. N. de S. Ribeiro, and M. V. Ribeiro, "An augmented capacitive coupling circuit for boosting plc systems in IoT domains," in *Proc. Symposium on Internet of Things*, pp. 1–5, 2023, doi: 10.1109/SIoT60039.2023.10390135.

[43] L. G. da S. Costa, A. C. M. de Queiroz, V. L. R. da Costa, and M. V. Ribeiro, "An analog filter bank-based circuit for performing the adaptive impedance matching in plc systems," *Journal of Communication and Information Systems*, vol. 36, no. 1, pp. 133–150, 2021, doi: 10.1109/TIM.2013.2280490.

Brazilian Microwave and Optoelectronics Society-SBMO   received 28 Oct 2023; for review 23 Nov 2023; accepted 23 Apr 2024

Brazilian Society of Electromagnetism-SBMag   © 2024 SBMO/SBMag   (cc) BY   ISSN 2179-1074

This document has an erratum: https://doi.org/10.1590/2179-10742024v23i3289482

Erratum received in 10 June 2024; revised in 15 July 2024; accepted in 13 Aug 2024.